AIAA JOURNAL
Vol. 38, No. 3, March 2000

Computation of Acoustic Propagation in Two-Dimensional Sheared Ducted Flows

Elisabeth Longatte* and Philippe Lafon†
Electricité de France, 92141 Clamart Cedex, France
and
Sébastien Candel‡
École Centrale Paris, 92295 Châtenay-Malabry Cedex, France

Most aeroacoustic noise-prediction methods rely on an acoustic analogy featuring a propagation equation associated with source terms. These models were mainly applied to computation of acoustic far fields radiated by simple free flows like jets. The assumption is made in many formulations that the radiated acoustic field is not perturbed by the shear flow giving rise to the noise sources. These acoustic analogies thus do not provide a full description of acoustic/flow interactions. The Lilley equation was introduced to account, to a certain extent, for mean shear effects on propagation. More recently, this problem has been treated by making use of the linearized Euler equations, which are more flexible and more adequate for numerical simulations. As several types of modes are supported by the Euler equations, problems linked to their coupling have to be considered. It is then necessary to investigate acoustic field computations in complex flows. Our aim in the present article is to validate the wave operator associated with linearized Euler equations. Numerical tests deal with propagation in two-dimensional sheared ducted flows. Results are compared with other solutions deduced from analytical developments and direct numerical simulations. This study shows that the linearized Euler operator may be used to account for mean effects on wave propagation in the presence of sheared ducted flows. Processes that are specifically considered are 1) convection effects on axial disturbances, 2) refraction effects on oblique wave generation, and 3) source radiation effects on propagation in sheared flows.

Nomenclature

c_0	= sound velocity
d	= duct width
L	= duct length
M	= Mach number
M_0	= duct centerline Mach number
p', p_a, p_b	= acoustic pressure, acoustic plane mode, acoustic oblique mode
p_0	= mean pressure
t, t'	= reduced and dimensional times
u', v'	= acoustic velocity disturbances
u_0, v_0	= mean velocity
x, y, x', y'	= reduced and dimensional space coordinates
Ω, ω'	= reduced and dimensional angular frequencies

I. Introduction

COMPUTATIONAL aeroacoustics (CAA) is a relatively new discipline combining acoustics and computational fluid dynamics (CFD). Whereas CFD methods are often used to solve spatial (time-independent) problems, CAA adds the temporal dimension requiring greater computational resources. Recent numerical developments have allowed gains in efficiency, and many difficulties have been overcome. Standard acoustic theories were primarily linear, assuming that perturbations were monochromatic, and most studies used uniform mean velocity, temperature, and sound speed profiles. These restrictions are not needed anymore. However, some problems remain that are related to acoustic source-term identification, to possible coupling between unstable modes and acoustic waves and to nonlinear interaction processes. In the following, we confine our attention to mean shear effects on acoustic wave propagation.

Most formulations of aeroacoustic problems feature a wave equation associated with source terms. In the framework of Lighthill's analogy, the propagation is described by a standard wave equation in a medium at rest, the second spatial derivative of the aerodynamic stress tensor providing acoustic source terms. This leads to an integral formulation of the sound field expressed in terms of the free-space Green's function corresponding to the wave operator. This analogy is well suited to free space radiation problems; nevertheless, it cannot account precisely for mean flow effects in complex cases. Furthermore, in confined configurations this method may involve numerical difficulties as it requires an adaptation of Green's functions to the specific geometry. It is then more appropriate to use the Euler equations to deal with acoustic/flow interactions.[1] The problem may be treated in three steps:

1) The mean flow is first determined (numerically) by solving the time-average Navier–Stokes equations associated with a turbulence closure scheme like the k–ϵ model.

2) Acoustic source terms related to the turbulent fluctuations are then synthesized by stochastic techniques.[2]

3) Finally, the source terms are incorporated in the right-hand side of the linearized Euler equations (LEE), which are solved in space and time.

The work of Goldstein shows that the linearized Euler system is equivalent to the Lilley's equation when the flow is simply stratified.[3] Now, both formulations, LEE and Lilley's equation, support acoustic and convective (vortical) disturbances. Clearly there is a possibility of coupling between these types of modes, and it is then logical to inquire whether the LEE properly account for acoustic mean/flow interactions including convection and refraction effects.

The present paper deals with this issue in the case of confined flows. To allow simple interpretations, the geometry of the problem has been simplified to the extreme. The purpose here is to understand propagation processes and related energy transfer. The cases under test are chosen to emphasize situations involving exchanges between mean quantities and acoustic modes. They concern

Presented as Paper 97-1631 at the AIAA/CEAS 3rd Aeroacoustics Conference, Atlanta, GA, 12–14 May 1997; received 13 August 1998; revision received 13 August 1999; accepted for publication 16 August 1999.

*Research Student, Département Acoustique et Mécanique Vibratoire, 1, Avenue du Général de Gaulle.

†Research Scientist, Département Acoustique et Mécanique Vibratoire, 1, Avenue du Général de Gaulle. Member AIAA.

‡Professor, Laboratoire EM2C, Centre National de la Recherche Scientifique. Member AIAA.

interactions between monochromatic acoustic waves and fully developed subsonic mean flow profiles.

Acoustic wave propagation in confined sheared flow was first studied by Pridmore-Brown,[4] who introduced and solved a second-order linearized equation:

$$\frac{1}{c_0^2}\frac{\partial^2 p'}{\partial t'^2} = (1-M^2)\frac{\partial^2 p'}{\partial x'^2} + \frac{\partial^2 p'}{\partial y'^2} - \frac{2M}{c_0}\frac{\partial^2 p'}{\partial t'\partial x'} + 2\rho_0 c_0 \frac{\mathrm{d}M}{\mathrm{d}y'}\frac{\partial v'}{\partial x'} \tag{1}$$

where x' and y' designate dimensional space coordinates and t' the real time, using conventions of Wang and Kassoy.[5] This equation governs propagation in a flow characterized by a mean Mach number $M = U/c$ and a density ρ_0. The fluid is stratified in the y direction, and the flow is adiabatic. Pressure perturbations are isentropic and related to density perturbations by $p' = c^2\rho'$. Equation (1) features the velocity fluctuation v', which is itself related to the pressure by the linearized momentum equation. It is solved by semianalytical techniques, and modal solutions are sought of the form

$$p(x', y', t') = F(\kappa, y')\exp[i(\kappa k_0 x' - \omega t')]$$

where F designates cross-stream eigenfunctions; $\kappa = c_0/v_{\mathrm{ph}}$ is the corresponding eigenvalue, and the reference wave number is defined as $k_0 = \omega_0/c$. These solutions take into account changes of axial wave number induced by convection and refraction in the presence of nonuniform mean flow. They feature the expected patterns describing downstream and upstream propagation as well as acoustic intensity distribution through the duct. They were thoroughly studied by Munger and Gladwell[6] and by Hersch and Catton,[7] among many others. However, these studies rely on restrictive assumptions and cannot predict the temporal evolution of an initial disturbance towards a modal form. Source radiation and refraction effects on oblique wave generation cannot be treated in this framework. More recently, Wang and Kassoy[5] proposed new analytical developments and interpretations taking into account transient responses and resonant conditions. Perturbation procedures were carried out for solving initial boundary-value problems and describing processes associated with acoustic generation and propagation. Using direct numerical simulation (DNS) (with the full Navier–Stokes equations), Mu and Mahalingam[8] provided original numerical solutions in agreement with experimental predictions and theoretical developments.

In this paper, we confirm these results by using another approach relying on the computation of LEE. After a brief formulation of the problem and a description of numerical methods and test cases, we discuss results of calculations by using qualitative and quantitative comparisons of numerical and analytical solutions.

II. Problem Formulation

A. Model Problem

We solve the LEE associated with a known subsonic mean flow, at high Reynolds number, which ensures that viscosity effects can be neglected. The system to be solved can be written as follows[9]:

$$\frac{\partial p'}{\partial t} + (\boldsymbol{u}_0\cdot\nabla)p' + (\boldsymbol{u}'\cdot\nabla)p_0 + \gamma p_0(\nabla\cdot\boldsymbol{u}') + \gamma p'(\nabla\cdot\boldsymbol{u}_0) = 0 \tag{2}$$

$$\frac{\partial \boldsymbol{u}'}{\partial t} + (\boldsymbol{u}_0\cdot\nabla)\boldsymbol{u}' + (\boldsymbol{u}'\cdot\nabla)\boldsymbol{u}_0 + \frac{1}{\rho_0}\nabla p' - \frac{p'}{\rho_0^2 c_0^2}\nabla p_0 = \boldsymbol{S} \tag{3}$$

where $\boldsymbol{u}'$, p' are dimensional quantities describing flow disturbances. S_u and S_v correspond to acoustic source terms associated with flow turbulence. These terms are not included here as we focus our attention on wave propagation. Mean pressure and velocity are designated as p_0, u_0, and v_0. To deal with propagation in sheared ducted flows, we consider a two-dimensional geometry (Fig. 1), assuming that the mean velocity profile is parallel, taking $v_0 = 0$ and $u_0(x, y) = U(y)$ with

$$U(y) = 4M_0 y(1-y)$$

The reduced spatial coordinate y is defined by $y = y'/d$, where d is the duct width. The duct aspect ratio is defined by $\alpha = d/L$; in what follows, we take $M_0 = 0.08$ and $\alpha = 5$. Duct walls are perfectly rigid, whereas nonreflecting conditions and artificial damping are imposed at the outlet to avoid spurious reflections and simulate infinite duct length. It is interesting to compare the frequency f of monochromatic disturbances imposed at the inlet to the cutoff frequencies of the duct without mean flow: $f_m^c = mc/2d$. The mth mode is propagative if $f > f_m^c$. When the Mach number M_0 is not too large, this condition will be approximately satisfied. To allow comparisons with previous work, we use the reduced angular frequency $\Omega = \omega' d/c$, which may be related to f and to the first mode cutoff frequency by $\Omega = \pi f/f_1^c$.

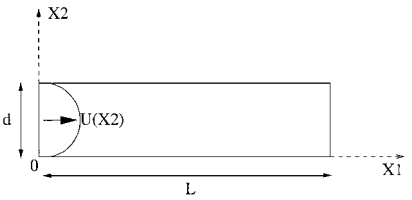

Fig. 1 Mean flow profile $U(y)$. Inlet disturbances are imposed in section $x = 0$, and nonreflecting conditions in section $x = L$.

B. Numerical Methods

The solution of the problem may be obtained by integrating a system of equations that can be cast in the compact form:

$$\frac{\partial \boldsymbol{W}}{\partial t} + \boldsymbol{A}\cdot\frac{\partial \boldsymbol{W}}{\partial \boldsymbol{X}} + \boldsymbol{B}\cdot\boldsymbol{W} + \boldsymbol{C} = 0 \tag{4}$$

with $\boldsymbol{W} = [p', u', v']^t$ and matrices $\boldsymbol{A}$, $\boldsymbol{B}$, and $\boldsymbol{C}$ easily deduced from Eqs. (2) and (3). Two general classes of numerical schemes may be used to deal with this system:

1) The first class relies on a weak formulation of linear equations. The key point of this method is that, in contrast with classical finite element methods, test functions are time dependent and evolve along the characteristic paths. Using splitting techniques, equations are solved in each direction of propagation. One-dimensional problems are then treated in space and time. This approach was implemented a few years ago at Electricité de France (EDF), and applications to aeroacoustic problems were thoroughly discussed by Esposito[10] and Bécharaet al.[1] The method features reduced levels of dissipation and dispersion. It requires, however, relatively large computational resources for the treatment of three-dimensional configurations.

2) Other numerical schemes were developed and have become standard in CAA. They are based on finite difference dispersion relation preserving schemes (DRP) devised by Tam and Webb.[11] We use in this study one such sixth-order scheme associated with a fourth-order Runge–Kutta temporal procedure. A strong characteristic method with three-point stencil is used for the treatment of boundaries, and an absorbing domain is introduced together with nonreflecting outflow conditions. The Courant–Friedrichs–Lewy (CFL) criterion must be satisfied to obtain a proper solution, and at least seven grid points are needed per wavelength.

Both schemes are now implemented in the Eole code developed by EDF. Results of both methods are in excellent agreement.

C. Nature of Inlet Disturbances

We study the propagation of monochromatic disturbances through mean ducted flows to exhibit acoustic/flow interactions. The nature of inlet disturbances is chosen to show as clearly as possible convection, refraction, and source effects on propagation. To check our results, we use a comparison with analytical solutions of Wang and Kassoy[5] and with results of DNS obtained by Mu and Mahalingam.[8] Two kinds of harmonic disturbances are introduced (Fig. 2):

1) In the first case we impose a nonplane source to exhibit generation of oblique waves induced simultaneously by sources and refraction. The plane and the first transverse acoustic modes of the duct without flow are introduced with the same magnitude orders. Inlet conditions are given by

$$u'(y, t) = \epsilon U(y)\sin(\pi y)\sin(t) \qquad \text{with} \qquad U(y) = 4M_0 y(1-y) \tag{5}$$

where ϵ is the disturbance magnitude and t a reduced time defined by $t = t'\omega'$. This perturbation is somewhat artificial, but this input incorporating the shear-layer profile allows direct comparison of our results with those of Mu and Mahalingam.[8]

2) In the second case we impose the plane mode alone to emphasize refraction effects. Inlet conditions are then specified as

$$u'(y, t) = \epsilon M_0 \sin(t) \tag{6}$$

We note $A(y)$ as the disturbance magnitude, y dependent in the first case, uniform in the second one. Using both inlet conditions, our aim is to study mean shear effects on propagation, which implies an identification of acoustic propagating modes. Hence, to interpret our results, we decompose the numerical acoustic pressure p' into its main components, the plane mode p_a and the first transverse modes p_b:

$$p' = p_a + p_b + o(p_b)$$

These components are obtained numerically after Fourier transformation and spatial filtering. This allows direct comparisons with analytical expressions given by Wang and Kassoy in Ref. 5. Their theoretical solutions are built as follows. Linearized hyperbolic equations are written in a strained system of coordinates:

$$\bar{x} = \frac{x}{1 + M\tilde{U}_0} \qquad \text{with} \qquad \tilde{U}_0 = \int_0^1 U(y)\,\mathrm{d}y$$

The system is solved by means of a Laplace transform and provides analytical expressions of first- and second-order acoustic pressures designated as p_1 and p_2 (Ref. 5). However, this method suffers from a lack of generality because it relies on asymptotic appoaches. For this reason only simplified configurations can be considered analytically:

1) When the inlet disturbance magnitude A is y dependent, as in expression (5), the analytical treatment assumes that the mean flow is uniform. In this case expressions of p', p_a, and p_b describe the propagation of plane and nonplane modes introduced at the inlet. However, the analytical solution assumes that the flow acts as a bulk and includes only convection effects through the variable $\bar{x}$. Hence, source effects on generation of oblique waves are taken into account, but direct shear effects like refraction are not described.

2) In contrast, when A is constant, as in expression (6), the mean flow is not necessarily uniform, and p' may be written as $p' = p_a + p_b$, with the following decomposition: $p_a = p_1 + Mp_{2a}$ and $p_b = Mp_{2b} + \mathcal{O}(Mp_{2b})$. The axial mode p_a is decomposed into p_1 describing convection effects on axial propagation and Mp_{2a} associated with refraction effects induced by mean shear on axial propagation. The higher-order term Mp_{2b} is the superposition of nonplane components of pressure. In this case the computation of the second-order pressure $p_2 = p_{2a} + p_{2b}$ includes refraction effects by shear on axial wave propagation. In the analytical solution, second-order phenomena such as refraction effects on oblique waves are excluded.

Using these formulations, we show next that numerical solutions deduced from LEE and analytical results are in good agreement. Small quantitative differences come from the fact that analytical solutions cannot simultaneously take into account refraction and source effects on oblique wave generation. Qualitative interpretations may be given to understand all mechanisms involved.

To check the results, we also use another comparison (not shown here) with numerical calculations of Mu and Mahalingam[8] based on DNS. Good agreement is found except in the boundary-layer region. This comes from the fact that direct simulations are based on the Navier–Stokes equations, and the corresponding acoustic velocity field falls to zero near the wall. As our solutions are deduced from linearized Euler equations, the acoustic velocity does not vanish near the wall.

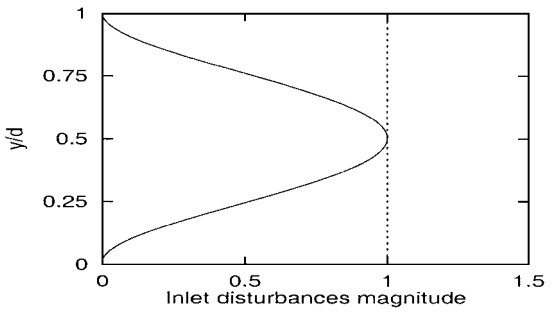

Fig. 2 Nature of inlet disturbances: ——, two first modes, and - - - -, plane mode.

III. Numerical Results and Comments

Many configurations have been tested by selecting different parameters, Mach number, ducted mean flow profile, frequency, magnitude, and nature of inlet disturbances. We here show results obtained for three different frequencies situated next and above the first cutoff frequency of the duct and near the second cutoff frequency. For the reduced frequency we successively take $\Omega = 2$, 8, and 2π. In each case solutions are evaluated numerically and analytically. Acoustic pressure time history, spatial distribution, and spectral contributions deduced from spatial spectral filtering are displayed in selected cases.

A. Below the First Cutoff Frequency

For a reduced frequency $\Omega = 2$ below the first cutoff frequency f_1^c of the duct without flow, the plane mode is dominant. Figure 3

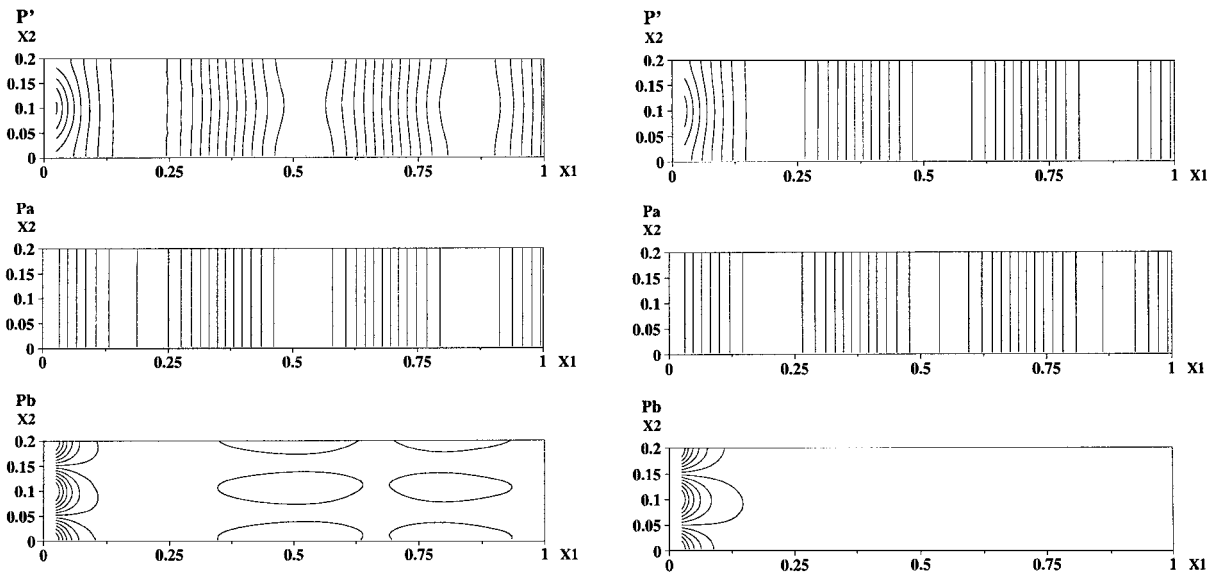

Fig. 3 Components of acoustic first modes evaluated numerically (left) and analytically (right): full solution (top), plane mode p_a (middle), and nonplane mode p_b (bottom) for $\Omega = 2$, with two modes at the inlet.

displays a modal distribution of acoustic pressure components when the first two modes are excited at the inlet. Acoustic waves are nearly axial, and the first transverse mode p_b computed analytically decreases quickly and becomes negligible at a sufficient distance from the inlet. In this case the analytical solution describes axial wave propagation but does not include refraction effects. In contrast, the numerical solution features the second-order mode caused by refraction of axial waves, and this mode is still present at a distance from the inlet.

When the plane mode is introduced alone at the inlet for this frequency, the plane mode p_a propagates through the duct without distorsion. Numerical and analytical solutions are in good agreement as shown by the time records of pressure (Fig. 4). As already mentioned, the analytical formulation used in this case takes simultaneously into account propagation of the plane mode introduced at the inlet and small refraction effects induced by shear. Hence, the analytical solution describes the same processes as the numerical one, except for second-order interactions, that is to say, refraction of oblique waves. According to these results, these processes may be neglected at this frequency.

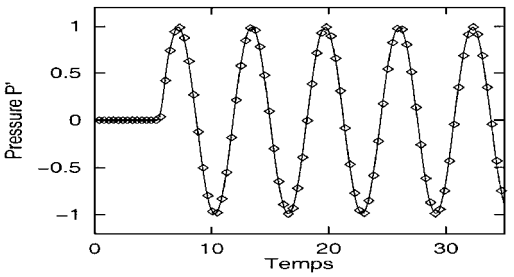

Fig. 4 Acoustic pressure time history evaluated numerically (——) and analytically (- - - -) at centerline for $\Omega = 2$ and at $x = \lambda$ with the plane mode at the inlet.

B. Above the First Cutoff Frequency

For $\Omega = 8$, just above the first cutoff frequency corresponding to the tranverse mode $m = 2$, oblique waves can propagate. With two modes at the inlet, the following processes take place: 1) oblique wave generation by refraction of downstream propagating waves caused by mean shear and 2) oblique wave generation caused by the structure imposed at the inflow. Figure 5 exhibits time histories of total acoustic pressure evaluated numerically and analytically at the wall and at centerline in section $x = \lambda$. This may be compared to Fig. 5 of Mu and Mahalingam.[8] In both results pressure histories differ at the wall and at the centerline indicating that the second tranverse mode develops. Modal distributions of pressure components p', p_a, and p_b are given in the spatial domain (Fig. 6) and along the centerline (Fig. 7). One can deduce the following qualitative informations about mode patterns. The plane mode p_a is not affected by refraction, and its magnitude is of the same order as in the case $\Omega = 2$, whereas the second-order pressure p_b supports all refraction effects and is of the same order as the plane mode in contrast with the case $\Omega = 2$. Here, the first two modes introduced at the inlet propagate downstream without attenuation. Whereas numerical and analytical plane modes are strictly similar, second-order pressures differ when the distance of propagation is greater than one wavelength. As refraction by shear is the only process neglected by the analytical computation of p_b, one may conclude that refraction by shear induces oblique wave generation.

Turning now to the downstream propagation of the plane mode introduced alone at the inlet for $\Omega = 8$, one observes new patterns. Time histories of acoustic pressure and of its main components are given in Fig. 8. Like in the case $\Omega = 2$, the plane mode is not affected by refraction, which appears only in the second-order pressure p_b. However, the magnitude of p_b is smaller than in the preceding case with two modes at the inlet. If one compares the results obtained for different values of the Mach number on the centerline, one can notice that p_b has a magnitude of order $\mathcal{O}(M)$ as expected by analytical developments of Wang and Kassoy.[5]

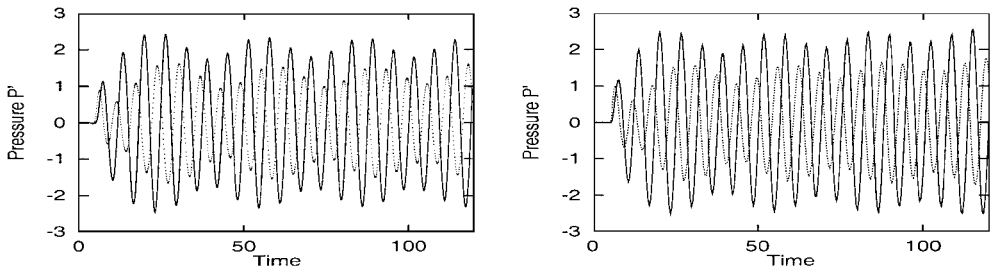

Fig. 5 Time history of pressure p' evaluated numerically (left) and analytically (right) at centerline (- - - -) and at wall (——) for $\Omega = 8$ and at $x = \lambda$ with two modes at the inlet.

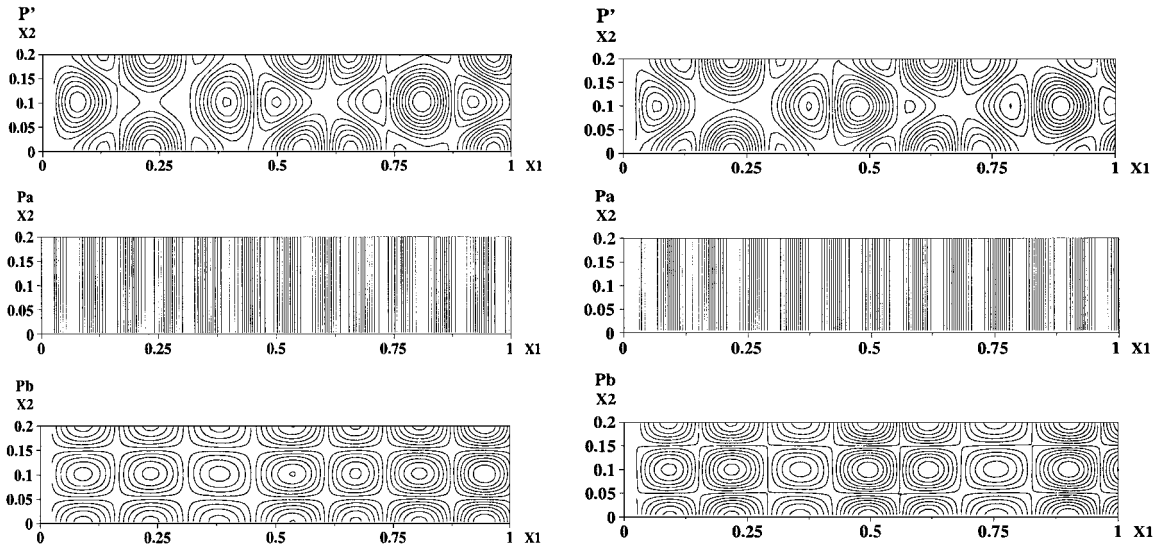

Fig. 6 Components of acoustic first modes evaluated numerically (left) and analytically (right): full solution (top), plane mode p_a (middle), and nonplane mode p_b (bottom) for $\Omega = 8$ with two modes at the inlet.

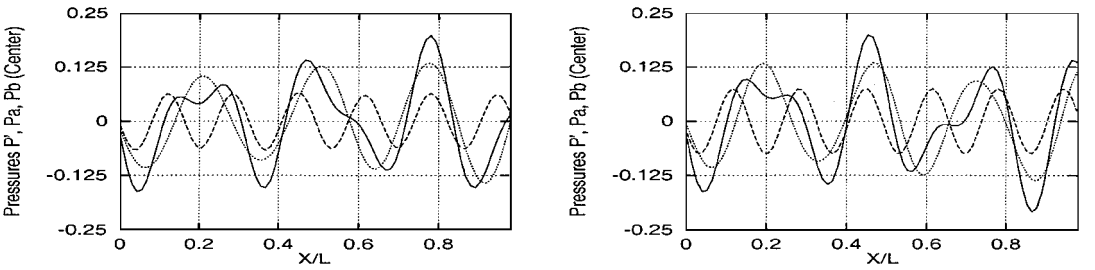

Fig. 7 Spatial propagation of pressures p' (——), p_a (· · · ·), and p_b (- - - -) evaluated numerically (left) and analytically (right) for $\Omega = 8$ at centerline with two modes at the inlet.

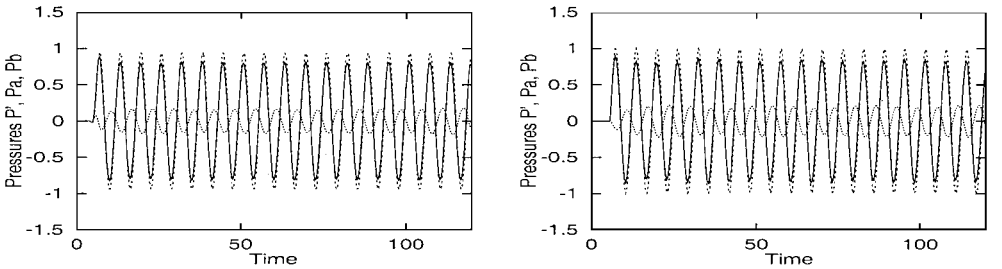

Fig. 8 Time history of pressures p' (——), p_a (· · · ·), and p_b (- - - -) evaluated numerically (left) and analytically (right) for $\Omega = 8$ at $x = \lambda$ with plane mode at the inlet.

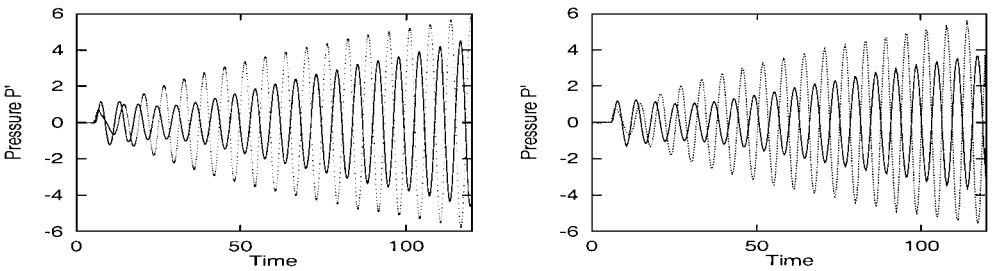

Fig. 9 Time history of pressure p' evaluated numerically (left) and analytically (right) at centerline (- - - -) and at wall (——) for $\Omega = 2\pi$ and at $x = \lambda$ with two modes at the inlet.

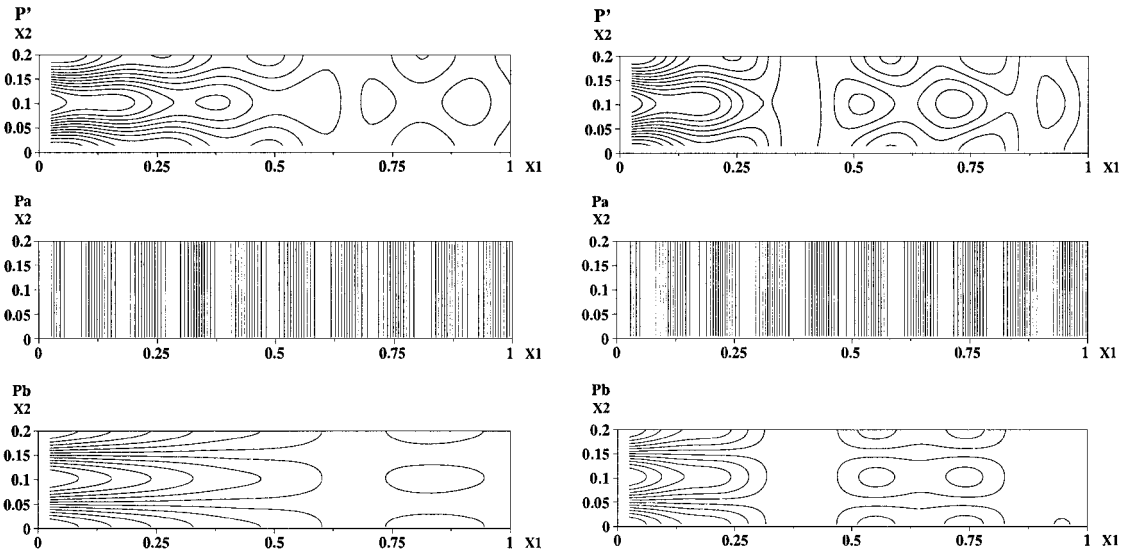

Fig. 10 Components of acoustic first modes evaluated numerically (left) and analytically (right): full solution (top), plane mode p_a (middle), and nonplane mode p_b (bottom) for $\Omega = 2\pi$ with two modes at the inlet.

C. Near the Second Cutoff Frequency

The last case corresponds to the reduced frequency $\Omega = 2\pi$ close to the second cutoff frequency of the duct without flow f_2^c corresponding to the second tranverse mode $m = 2$. Figure 9 displays the time history of pressure evaluated numerically and analytically in section $x = \lambda$; modal distributions are given in Fig. 10. The plane mode does not feature a resonant behavior, whereas the second-order pressure p_b is nearly resonant. The magnitude of p_b at a given location is modulated in time indicating that energy transfers occur from the boundary layer toward the duct center and conversely. These processes can be explained by interactions between axial waves and nearly transverse modes that are excited at resonant frequencies. Like in the case $\Omega = 8$, the two modes introduced at the inlet propagate without attenuation.

In the case of plane mode excitation for $\Omega = 2\pi$, the plane mode propagates without distorsion, whereas the second-order mode p_b

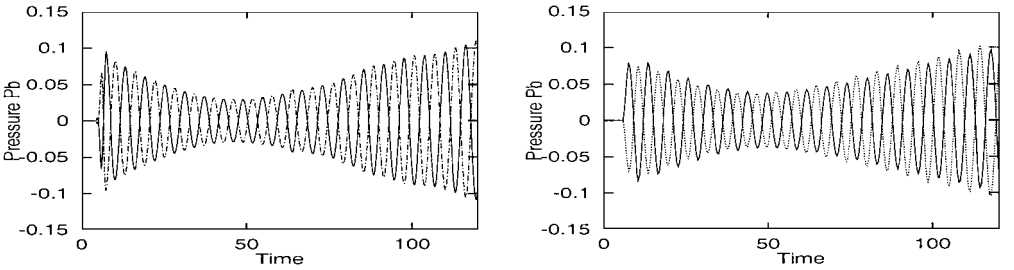

Fig. 11 Time history of pressure p_b evaluated numerically (left) and analytically (right) with $M = 0.08$ for $\Omega = 2\pi$ at $x = \lambda$ at centerline (- - - -) and at wall (——) with the plane mode at the inlet.

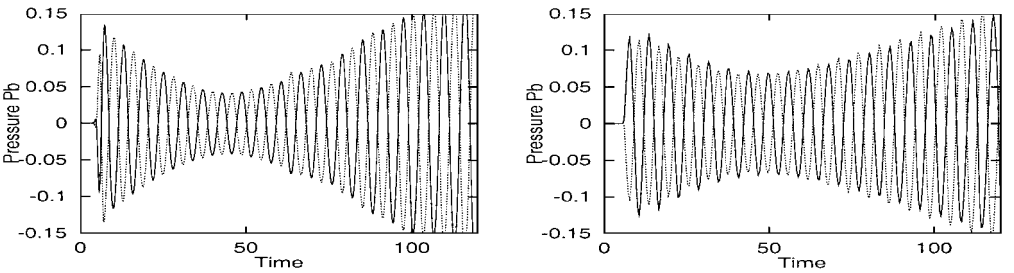

Fig. 12 Time history of pressure p_b evaluated numerically (left) and analytically (right) with $M = 0.12$ for $\Omega = 2\pi$ at $x = \lambda$ at centerline (- - - -) and at wall (——) with the plane mode at the inlet.

is nearly resonant. As expected in this case, the magnitude of p_b is much smaller than that of p and p_a. If one compares the results for different Mach number values (Fig. 11 for $M = 0.08$ and Fig. 12 for $M = 0.12$), one finds that numerical and analytical solutions are in good agreement over a long period. However, for $M = 0.12$ a difference arises beyond $t \sim 70$. According to Wang and Kassoy,[5] under resonant conditions p_b is of magnitude of order $\mathcal{O}(M)$ until t is of order of $\mathcal{O}(M^{-2})$. For large times the theoretical solution is invalid. Hence, numerical results are in good agreement with theoretical solutions, at least until the theoretical solution breaks down.

IV. Conclusions

The wave operator associated with LEE can be used to describe the propagation of acoustic disturbances through sheared ducted flows. Results are in good agreement with analytical theories and numerical solutions deduced from direct simulation. The LEE suitably describe mean shear effects on the distribution of acoustic intensity in ducts. Other calculations not shown here indicate that opposite effects of convection and refraction on downstream and upstream propagating waves are well calculated. Refraction effects on propagation and oblique wave generation are included. Effects of initial inlet distribution, frequency, and magnitude on transverse mode generation are displayed through modal decompositions. Transitions that may occur between propagating modes at resonant frequencies are well observed. Except for the acoustic boundary layer that is not included in our inviscid treatment and has to be explicitely introduced, all processes associated with acoustic propagation are well modeled.

This study provides a validation of acoustic fields computed in confined configurations. This is a first step in the analysis of coupling occuring between flows and waves originating from embedded noise sources. Acoustic-flow interactions may be significant as some vortical convective structures are supported by LEE and can develop or act on acoustic propagation when the velocity profile is unstable. Such cases will be developed in further studies related to noise generation by turbulence and relying on stochastic synthesis of acoustic source terms.

References

[1] Béchara, W., Bailly, C., Lafon, P., and Candel, S. M., "Stochastic Approach to Noise Modeling for Free Turbulent Flows," *AIAA Journal*, Vol. 32, No. 3, 1994, pp. 455–463.

[2] Bailly, C., Lafon, P., and Candel, S., "A Stochastic Approach to Compute Noise Generation and Radiation of Turbulent Flows," AIAA Paper 95-092, June 1995.

[3] Colonius, T., Moin, P., and Lele, S. K., "Direct Computation of Aerodynamic Sound," Stanford Univ., Rept. TF-65, Stanford, CA, June 1995.

[4] Pridmore-Brown, D. C., "Sound Propagation in a Fluid Flowing Through an Attenuating Duct," *Journal of Fluid Mechanics*, Vol. 4, 1958, pp. 393–406.

[5] Wang, M., and Kassoy, D. R., "Transient Acoustic Processes in a Low-Mach-Number Shear Flow," *Journal of Fluid Mechanics*, Vol. 238, 1992, pp. 509–536.

[6] Munger, P., and Gladwell, G. M. L., "Acoustic Wave Propagation in a Sheared Fluid Contained in a Duct," *Journal of Sound and Vibration*, Vol. 9, No. 1, 1969, pp. 28–48.

[7] Hersch, A. S., and Catton, I., "Effect of Shear Flow on Sound Propagation in Rectangular Ducts," *Journal of the Acoustical Society of America*, Vol. 50, No. 3, 1971, pp. 992–1003.

[8] Mu, S., and Mahalingam, S., "Direct Numerical Simulation of Acoustic/Shear Flow Interactions in Two-Dimensional Ducts," *AIAA Journal*, Vol. 34, No. 2, 1996, pp. 237–243.

[9] Lafon, P., "Computation of Waves Propagation in a Complex Flow," *ICASE/LaRC Workshop on Benchmark Problems in Computational Aeroacoustics*, Inst. for Computer Applications in Science and Engineering, Hampton, VA, 1995, pp. 125–129.

[10] Esposito, P., "A New Numerical Method for Wave Propagation in a Complex Flow," *Numerical Methods in Laminar and Turbulent Flow*, Vol. 5, edited by C. Taylor, W. G. Habashi, and M. M. Hafez, Pineridge, Swansea, Wales, U.K., 1987, pp. 1315–1326.

[11] Tam, C. K. W., and Webb, J. C., "Dispersion-Relation-Preserving Finite Difference Schemes for Computational Acoustics," *Journal of Computational Physics*, Vol. 107, No. 2, 1993, pp. 262–281.

P. J. Morris
Associate Editor